Chinese Journal of Chemical Engineering xxx (xxxx) xxx–xxx

Contents lists available at ScienceDirect

Chinese Journal of Chemical Engineering

journal homepage: www.elsevier.com/locate/CJChE

Article

Selective synthesis of triacetin from glycerol catalyzed by HZSM-5/MCM-41 micro/mesoporous molecular sieve☆

Jiangyong Liu [1,*], Zihao Wang [1], Yunlin Sun [1], Ruiqi Jian [2], Panming Jian [1], Dan Wang [3,*]

[1] School of Chemistry and Chemical Engineering, Yangzhou University, Yangzhou, 225002, China
[2] School of Medicine, Stanford University, Stanford, CA 94304, USA
[3] State Key Laboratory of Organic-Inorganic Composites, Beijing University of Chemical Technology, Beijing 100029, China

ARTICLE INFO

Article history:
Received 16 May 2018
Received in revised form 4 September 2018
Accepted 11 September 2018
Available online xxxx

Keywords:
Mesoscale
Porous materials
Molecular sieve
Triacetin
Glycerol esterification

ABSTRACT

HZSM-5/MCM-41 molecular sieve (H-ZM) catalysts with well-defined micro/mesoporous structures were synthesized and showed high performance for selective synthesis of triacetin *via* the esterification reaction of glycerol with acetic acid. The conversion of glycerol was demonstrated to be 100% and the triacetin selectivity was over 91%, which can be attributed to the synergistic effect regarding suitable acidic property, excellent diffusion efficiency and good stability derived from the combined advantages of microporous molecular sieve HZSM-5 and mesoporous molecular sieve MCM-41.

1. Introduction

Glycerol, the main byproduct in the biodiesel, has resulted in a drastic surplus in the chemical market due to the ever-increasing production and demand of biodiesel [1–4]. Green chemical engineering including the design of chemical processes [5] and efficient catalysts [6] for green product and green process, has been regarded as one of the most efficient means of achieving sustainable development in chemical industry [7]. To date, extensive research efforts have been focused on the methods to transform glycerol into high value-added chemicals [8–11]. Among them, the acid-catalyzed esterification of glycerol with acetic acid (EGAA) for glycerol conversion into monoacetyl glycerol (monoacetin, MAG), diacetyl glycerol (diacetin, DAG) and triacetyl glycerol (triacetin, TAG) has aroused much attention both in the academic community and industrial field (Fig. 1) [1,2,11–13].

Although various catalysts, especially the heterogeneous acid catalysts, have been applied in the EGAA reaction, the low selectivity of the desired products (DAG and TAG) remains the greatest challenge in this reaction [2,14]. In addition, the recovery of the key derivatives is complicated since the products have comparable boiling points [15]. Among the three glycerol esters, TAG, as an important fuel additive, antimicrobial and emulsifying agent in pharmaceuticals and cigarette filters [16], however, is the most difficult to produce [1,17]. Microporous molecular sieves with unique pore structure, acidity feature and high stability [18–20], were employed in the EGAA reaction [21,22]. However, the reaction performances of these catalysts were very poor with the selectivity of TAG generally lower than 30%, which can be attributed to the diffusion difficulty of the acetylated esters within the microporous channels. Even loading the ultra-stable Y zeolite with dodecamolybdophosphoric acid, the result was still unsatisfactory [23]. Although the mesoporous molecular sieves with well-defined mesoporous structure, large pore size and high surface area [24–26], they were usually used as the catalyst supports in the EGAA reaction due to the lacking of necessary acidic sites. For example, 12-tungstophosphoric acid/MCM-41 [27], molybdophosphoric acid/SBA-15 [28], and SO_3H-SBA-15 [29] have showed improved catalytic performance as compared with the microporous molecular sieves. However, these catalysts cannot achieve a high catalytic activity and TAG selectivity at the same time.

In this article, we report the synthesis of well-defined HZSM-5/MCM-41 micro/mesoporous molecular sieve (H-ZM) composites which can serve as efficient catalyst for the selective synthesis of TAG *via* the EGAA process. The H-ZM catalysts combine the advantages of HZSM-5 and MCM-41, providing suitable acidic property, excellent diffusion efficiency and good stability, resulting in high catalytic performance. The effects of influencing factors including reaction time, catalyst amount and n(AcOH)/n(glycerol) on the catalytic performance were systematically investigated.

☆ Supported by the National Natural Science Foundation of China (21620102007), the Natural Science Foundation for High Education of Jiangsu Province (17KJB530011), the Science and Technology Innovation Foundation of Yangzhou University (2017CXJ015), and the Priority Academic Program Development of Jiangsu Higher Education Institutions (PAPD).
* Corresponding authors.
E-mail addresses: liujy@yzu.edu.cn (J. Liu), wangdan@mail.buct.edu.cn (D. Wang).

https://doi.org/10.1016/j.cjche.2018.09.013
1004-9541/

Please cite this article as: J. Liu, *et al.*, Selective synthesis of triacetin from glycerol catalyzed by HZSM-5/MCM-41 micro/mesoporous molecular sieve, *Chin. J. Chem. Eng.* (2018), https://doi.org/10.1016/j.cjche.2018.09.013

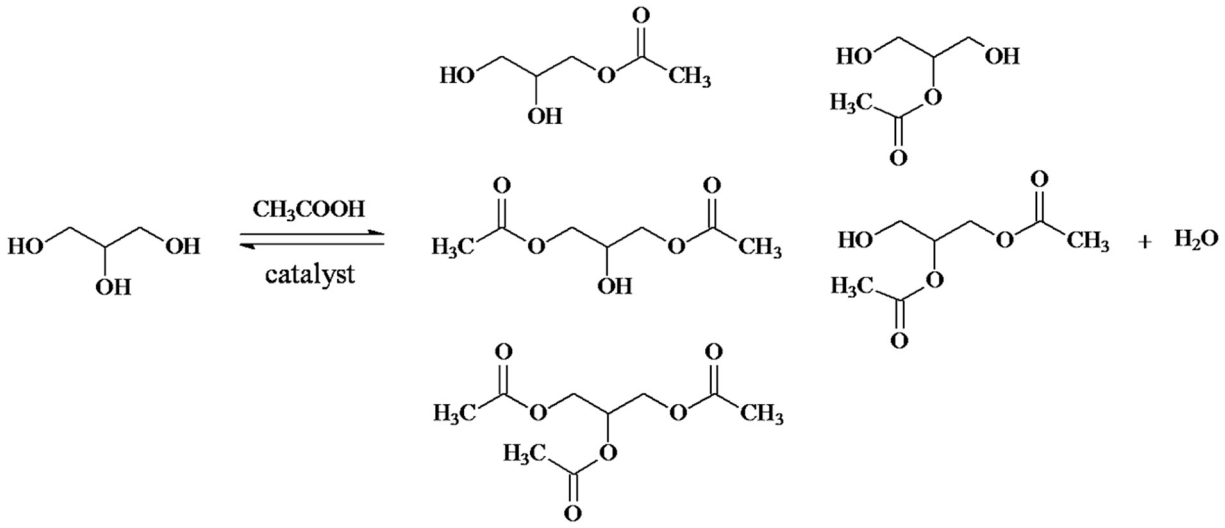

Fig. 1. Reaction scheme for the catalytic esterification of glycerol with acetic acid.

2. Experimental

2.1. Preparation of the catalysts

All the reagents were used as received without further purification. In a typical experiment, 2.0 g ZSM-5 powder and 15 ml NaOH aqueous solution (0.5 mol·L^{-1}) were added to a 100 ml beaker under stirring for 1 h. Then 15 ml Na_2SiO_3 solution (0.25 mol·L^{-1}) and 17 g Cetyltrimethylammonium bromide (CTAB) solution (5.9 wt%) were added to the suspension with stirring for another 1 h. Thereafter, the suspension was transferred into a Teflon-lined stainless-steel autoclave and heated at 120 °C for 48 h. After cooling to room temperature, the pH of the reaction mixture was adjusted to 8.5 with l.0 mol·L^{-1} sulfuric acid solution. Afterwards, the mixture was allowed for crystallization with another 24 h. After crystallization, the sample was obtained by filtration and washed thoroughly with deionized water and ethanol. The solid product was dried at 100 °C for 6 h and calcined at 550 °C for 5 h, and thus the ZSM-5/MCM-41 (ZM) composite molecular sieve

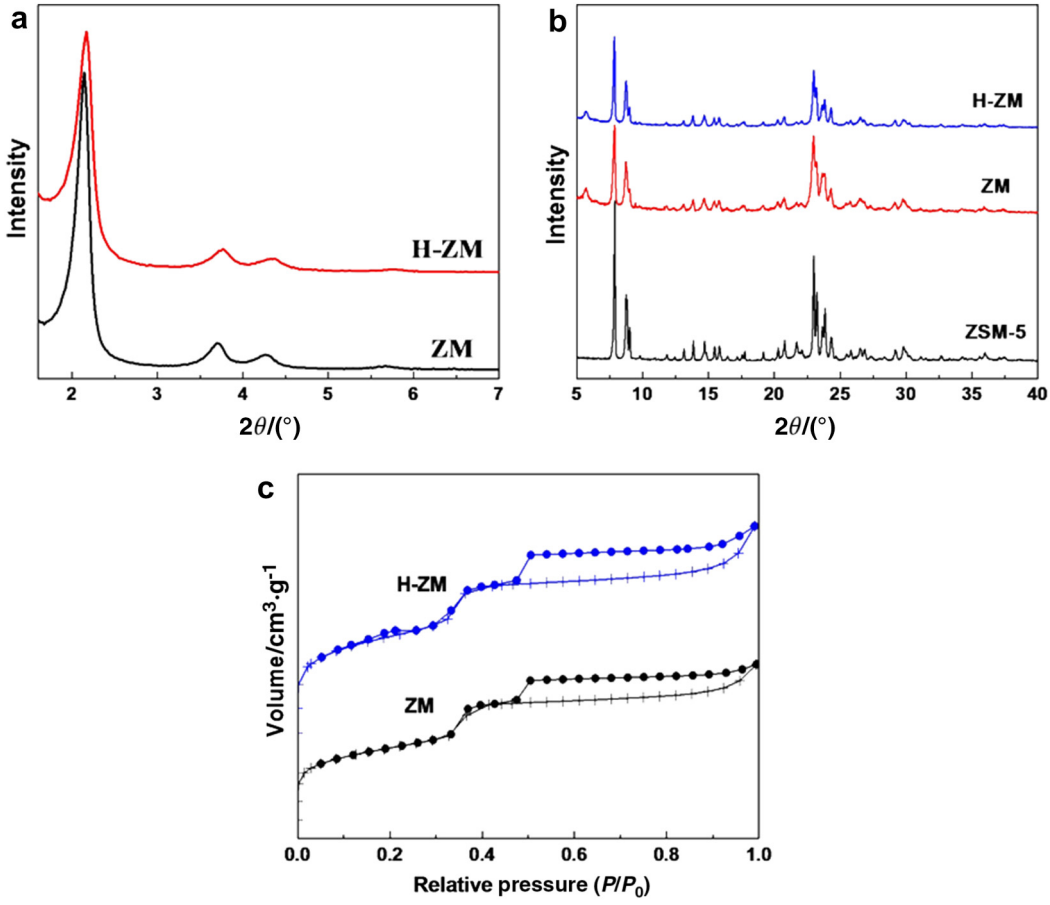

Fig. 2. Small-angle XRD patterns (a), wide-angle XRD patterns (b) and N_2 adsorption–desorption isotherms (c) of the samples.

Please cite this article as: J. Liu, *et al.*, Selective synthesis of triacetin from glycerol catalyzed by HZSM-5/MCM-41 micro/mesoporous molecular sieve, *Chin. J. Chem. Eng.* (2018), https://doi.org/10.1016/j.cjche.2018.09.013

was obtained. For the synthesis of proton-type HZSM-5/MCM-41 (H-ZM) composite molecular sieve, 4.5 g ZM sample was firstly added to 100 ml hydrochloric acid (0.1 mol·L^{-1}) in a 250 ml beaker, and the ion-exchange process was conducted for 8 h. And then the suspension was filtrated and washed with deionized water until the pH is neutral. The obtained product was then dried at 100 °C for 6 h before subjecting it for calcination at 550 °C for 2 h. The ion-exchange process was repeated for three times, and then the H-ZM micro/mesoporous molecular sieve was finally obtained.

2.2. Characterizations

The powder X-ray diffraction (XRD) was recorded on a Bruker D8 Advance diffractometer using Cu K_α radiation ($\lambda = 0.154056$ nm). The Fourier-transform infrared (FT-IR) spectra of the samples within the spectral range 4000–400 cm^{-1} were obtained on a Bruker Tensor 27 spectrometer. The morphology and microstructure of the samples were investigated with scanning electron microscope (SEM, Hitachi S-4800) and transmission electron microscope (TEM, Philip Tecnai 12). The N_2 isothermal adsorption–desorption measurement was conducted with a Micromeritics ASAP 2020 system. Prior to the test, the samples were outgassed at 200 °C for 5 h. The surface area of the samples was determined by the Brunauer–Emmett–Teller (BET) method. The mesopore volume was calculated at a relative pressure (P/P_0) of about 0.99, where P and P_0 are the measured and equilibrium pressures, respectively. The mesopore size was measured with the Barrett–Joyner–Halenda (BJH) method. In addition, the micropore size was calculated by the Horvath–Kawazoe (HK) method, and the micropore volume was measured with the t-plot method. The NH_3-TPD experiment was performed on a Finetec FINESORB-3010 apparatus equipped with a thermal conductivity detector. Prior to the NH_3 adsorption, the samples were pretreated at 200 °C for 2 h in a flow of Ar and then cooled down to 100 °C. Afterwards, ammonia was introduced and maintained for 1 h. Finally, the desorption step was conducted in Ar with a heating rate of 10 °C·min^{-1}.

2.3. Catalytic analysis of the H-ZM

For the selective synthesis of TAG from the EGAA process, in a typical process, the catalyst, glycerol and acetic acid were added to a three-necked, round-bottomed flask quipped with a mechanical stirrer, a thermometer and a distillation column. During the reaction, the formed water was constantly removed to positively shift the chemical equilibrium. The esterification process was monitored by analyzing the product with gas chromatography using a flame ionization detector (FID) equipped with a SE-30 capillary column.

3. Results and Discussions

Fig. 2a shows the small-angle XRD patterns of the ZM and H-ZM samples. It can be observed that similar to the characteristic diffraction peaks of MCM-41, a strong diffraction peak at about 2.1°, and three lower intensity diffraction peaks at the higher diffraction angles present for both of the samples. These diffraction peaks correspond to the (100), (110), (200) and (210) crystal planes, indicating that the samples have a highly ordered hexagonal symmetry structure [30]. The wide-angle

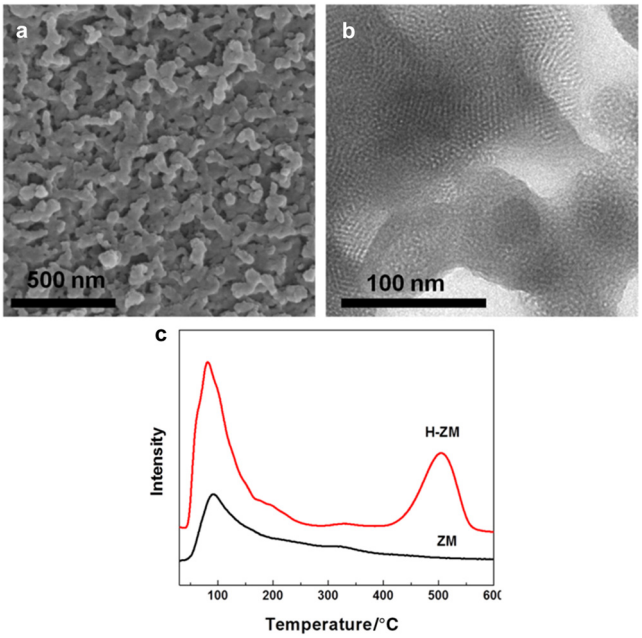

Fig. 3. Representative SEM image (a) and TEM image (b) of H-ZM, and the NH_3-TPD profiles (c) of the samples.

XRD patterns of ZM and H-ZM (Fig. 2(b)) show that the samples exhibit characteristic diffraction peaks of ZSM-5, but the peak intensities of the composite molecular sieves are lower than that of the pure ZSM-5 sample. This suggests that the ZM and H-ZM samples are composite materials with both the mesoporous structure of MCM-41 and microporous structure of ZSM-5. Additional information about the composite structure of ZM and H-ZM can be reflected from the FT-IR spectra of the samples (Fig. S1), where the band at about 550 cm^{-1} attributed to the asymmetric stretching vibration of SiO_4 tetrahedra is an important feature of ZSM-5 as a typical MFI type zeolite [31]. The pure MCM-41, however, has no band at 550 cm^{-1}, indicating that the soluble aluminosilicate species containing the fragments of the ZSM-5 structure had finally entered the mesoporous structure of MCM-41 in ZM and H-ZM. The N_2 adsorption–desorption isotherms of ZM and H-ZM (Fig. 2(c) and Table 1) show that the samples present fast adsorption at P/P_0 of 0–0.2, and have a small hysteresis loop at P/P_0 of 0.32–0.42 and a larger one at higher P/P_0, which is another evidence of the micro/mesoporous structure of ZM and H-ZM and is in accordance with the XRD and FT-IR results.

The SEM image of H-ZM (Fig. 3(a)) shows that the sample is composed of uniform irregular aggregates with the size of about 100 nm, and no typical morphology of ZSM-5 zeolite can be observed, which further confirms that the H-ZM sample is a composite molecular sieve but not a simple mechanical mixture of ZSM-5 and MCM-41. The TEM image of H-ZM (Fig. 3(b)) also illustrates a highly ordered mesopore organization of the sample, and is in line with the small-angle XRD result. The acidic property of ZM and H-ZM were investigated by the NH_3-TPD experiment (Fig. 3(c)). The NH_3-TPD profile of ZM shows only one peak, corresponding to the desorption of NH_3 from the weak acidic sites, while the intensity of this peak is significantly improved in H-ZM. In

Table 1
Texture parameters of the samples

Sample	2θ/(°)	d_{100}①/nm	a_0/nm	d_w②/nm	Pore size/nm		Pore volume/cm^3·g^{-1}		S_{BET}/m^2·g^{-1}
					Mesopore (d_p)	Micropore	Mesopore	Micropore	
ZM	2.12	4.16	4.80	1.95	2.85	0.50	0.37	0.084	500
H-ZM	2.17	4.07	4.70	1.86	2.84	0.51	0.37	0.086	501

① Lattice parameter for a hexagonal structure: $a_0 = 2d_{100}/\sqrt{3}$.
② Thickness of pore wall: $d_w = a_0 - d_p$.

Please cite this article as: J. Liu, *et al.*, Selective synthesis of triacetin from glycerol catalyzed by HZSM-5/MCM-41 micro/mesoporous molecular sieve, *Chin. J. Chem. Eng.* (2018), https://doi.org/10.1016/j.cjche.2018.09.013

addition, another desorption peak centered at about 500 °C ascribed to the strong acidic sites appears in H-ZM, indicating more and stronger acidic sites were generated for H-ZM after the ion-exchange process of ZM.

The acidic H-ZM catalyst was employed for the selective synthesis of TAG from the EGAA process, and the effects of influencing factors including reaction time, catalyst amount and n(AcOH)/n(glycerol) on the catalytic performance were systematically investigated. In the absence of catalyst, although the conversion of glycerol reached 47.7% after 24 h, the undesired MAG accounted for 82.1% of the product and only very little of TAG was generated (Table 2). Fig. 4a shows the effect of reaction time on the catalytic performance, suggesting that the glycerol conversion reached 93% within 2 h and 100% in 10 h. For the glycerol esterification process, acetic acid could selectively attach any hydroxyl groups (—OH) in the glycerol backbone or any —OH from the partially reacted glycerides. At the initial stage, glycerol was converted mostly to MAG and DAG. As the reaction progressed, MAG and DAG were gradually transformed into TAG (Fig. S2) that is the most difficult to produce in the three-step reaction of glycerol esterification due to the steric hindrance effect [32]. The TAG selectivity reached as high as 88.9% in 32 h and 91.3% in 48 h with 100% glycerol conversion, which is much better than the recent reports with the TAG selectivity of 71% (Keggin-type heteropolyacid catalysts) [12], 42% ($Fe_4(SiW_{12}O_{40})_3$ catalyst) [33], 57% (Sulphonated hydrothermal carbon catalyst) [34] and 29.2% (SO_4^{2-}/γ-Al_2O_3 catalyst) [35].

Table 2
Comparison of the catalytic performance of different catalysts[①]

Catalyst	Conversion/%	Selectivity/%		
		MAG	DAG	TAG
blank	47.7	82.1	16.7	1.2
MCM-41	70.5	76.4	19.8	3.8
HZSM-5	88.2	76.1	15.7	8.2
ZM	92.6	55.9	23.4	20.7
H-ZM	100	0.20	17.9	81.9

① Reaction conditions: 0.15 mol glycerol, 1.20 mol acetic acid, 1.5 g catalyst, 24 h, 125 °C.

Previous studies show that the key role of solid acid catalysts in the EGAA process depends on the acidity, texture and surface morphology of the catalyst [12,28,36,37]. In addition, the diffusion efficiency of the reactants and products is also of vital importance for the high rate of glycerol conversion and selective formation of DAG and TAG as both products, especially the latter, which is space demanding for the diffusion within the catalyst pores [2,21,38]. Table 2 lists the catalytic performances of the MCM-41, HZSM-5 and ZM for comparison, which can well confirm the importance of catalyst acidity and diffusion efficiency in the EGAA process oriented to the production of higher esters. Therefore, the superb catalytic performance of the H-ZM catalyst as compared with its counterparts for the EGAA reaction can be attributed to the synergistic effect regarding suitable acidic property, excellent diffusion efficiency and good stability derived from the composite structure of H-ZM that can effectively integrate the advantages of microporous molecular sieve HZSM-5 and mesoporous molecular sieve MCM-41. These merits of the H-ZM catalyst provide numerous acidic sites, high surface area and confined reaction environment for the direct synthesis of TAG by the EGAA process. Considering that the TAG selectivity had only tiny change after 32 h, we chose 32 h as the optimal reaction time for the investigation of other influencing factors. Fig. 4(b) exhibits the effect of catalyst amount (0.5–2.5 g) on the catalytic performance. As observed, the catalyst amount had no effect on

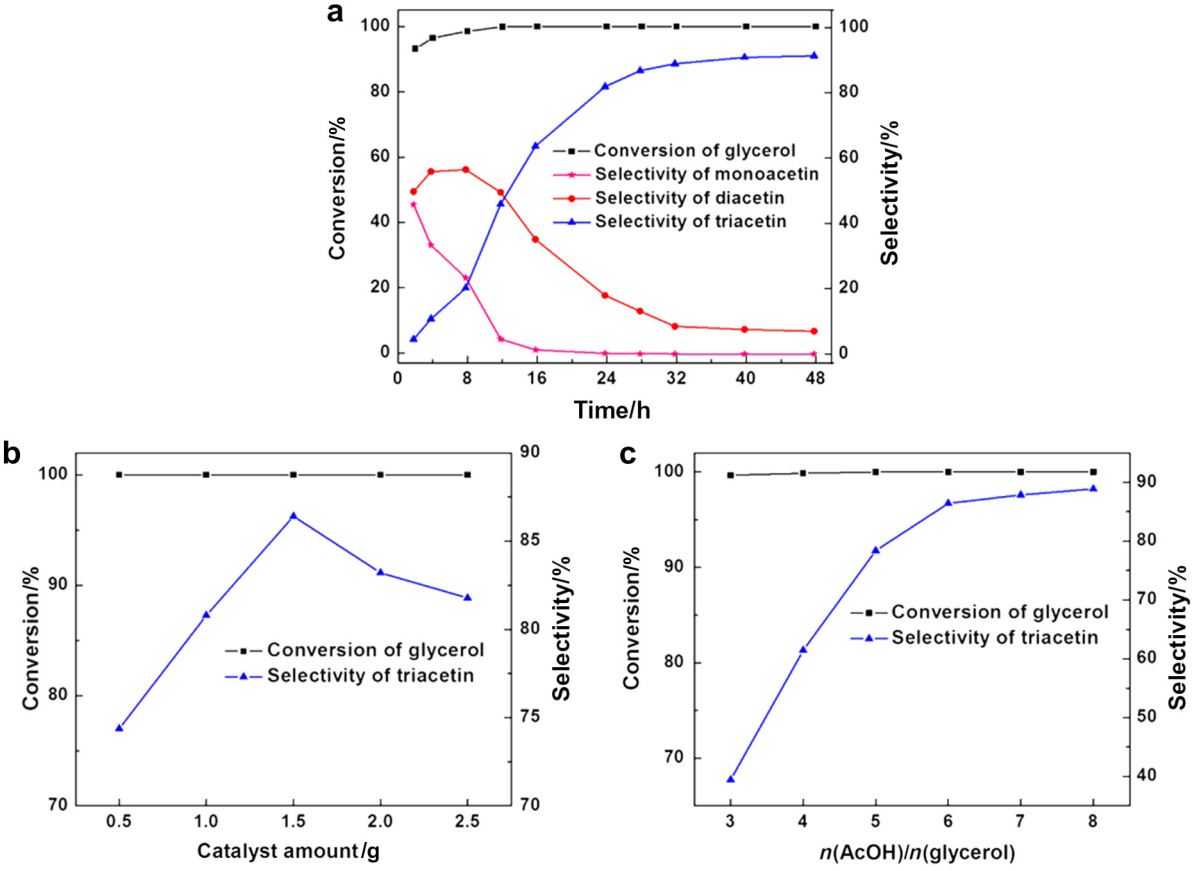

Fig. 4. (a) The effect of reaction time on the catalytic performance of the EGAA process. Reaction condition: 0.15 mol glycerol, 1.20 mol acetic acid, 1.5 g H-ZM, 125 °C. (b) The effect of catalyst amount on the catalytic performance. Reaction condition: 0.15 mol glycerol, 1.20 mol acetic acid, 32 h, 125 °C. (c) The effect of molar ratio of acetic acid and glycerol [n(AcOH)/n(glycerol)] on the catalytic performance. Reaction condition: 0.15 mol glycerol, 1.5 g H-ZM, 32 h, 125 °C.

Please cite this article as: J. Liu, *et al.*, Selective synthesis of triacetin from glycerol catalyzed by HZSM-5/MCM-41 micro/mesoporous molecular sieve, *Chin. J. Chem. Eng.* (2018), https://doi.org/10.1016/j.cjche.2018.09.013

the glycerol conversion but significant effect on the TAG selectivity. The highest TAG selectivity was achieved with the H-ZM amount of 1.5 g, indicating that most suitable number of accessible active sites were available for the deepest conversion of glycerol to TAG at this catalyst amount while further increase beyond 1.5 g would accelerate the generation of by-products [39]. The effect of n(AcOH)/n(glycerol) (3.0–8.0) on the esterification performance was studied as well, and the results were presented in Fig. 4(c).

Theoretically, at least 3 mol acetic acid is required to react completely with 1 mol glycerol to produce TAG. However, it can be expected that the excessive acetic acid should be used to positively shift the chemical equilibrium and achieve the higher selectivity of TAG [1]. Despite the 100% conversion of glycerol, the TAG selectivity constantly increased with increasing the n(AcOH)/n(glycerol). In addition, the TAG selectivity did not apparently increase at molar ratios higher than 6, indicating the occurrence of saturation [27]. Therefore, n(AcOH)/n(glycerol) of 6 was selected as the optimal reaction condition. Catalyst stability and the feasibility of reuse are key attractions to robust heterogeneous catalysts and is one of the most important parameters to commercialize the catalyst [40]. To that end, the durability test of the H-ZM catalyst was performed and presented in Fig. 5, indicating that the catalytic stability can be well reserved with no obvious decrease in the catalytic activity and TAG selectivity over four cycles. After reaction, the spent H-ZM catalyst still displays a good textural mesoporosity (Fig. S3).

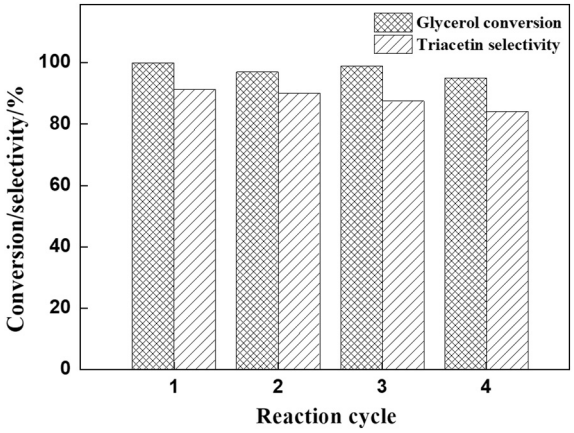

Fig. 5. Evaluation of the durability of H-ZM as the catalyst for the EGAA process.

Furthermore, we chose the esterification of ethylene glycol with acetic acid (Fig. 6) as another esterification reaction to test the catalytic performance of the H-ZM catalyst. The reaction condition is similar with that of the EGAA process except that the reactant composition in the flask is 0.25 mol ethylene glycol, 0.75 mol acetic acid and 0.7 g H-ZM. The reaction results (Fig. 7) show that a high yield of ethylene glycol diacetate as the target product can be achieved, indicating that the H-ZM catalyst is also effective in this reaction.

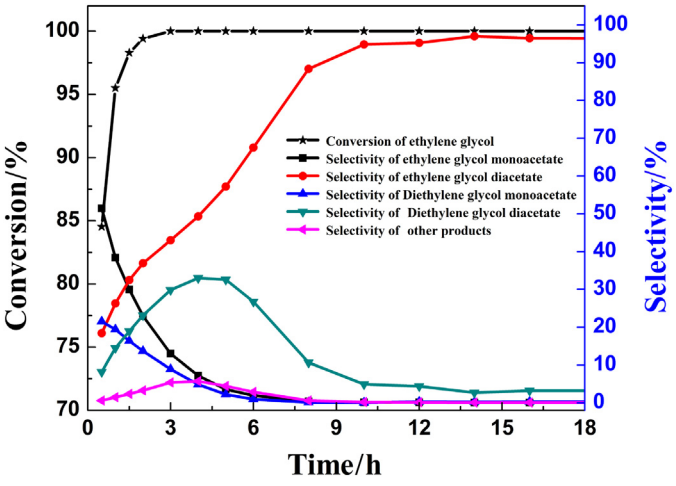

Fig. 7. The esterification of ethylene glycol with acetic acid using the H-ZM catalyst.

4. Conclusions

In conclusion, the HZSM-5/MCM-41 micro/mesoporous molecular sieve was prepared and employed as an efficient catalyst for the selective synthesis of TAG from the EGAA process. The H-ZM catalyst exhibits remarkable catalytic performance with glycerol conversion of 100% and TAG selectivity of 91.3%, which can be ascribed to the suitable acidic property, excellent diffusion efficiency and good stability due to the combined advantages of microporous molecular sieve HZSM-5 and mesoporous molecular sieve MCM-41. These unique features of the H-ZM catalyst ensures numerous acidic sites, high surface area and confined reaction environment for the highly selective synthesis of TAG. In addition to the excellent reaction performance, the environmental benignity and cost-effectiveness also make the H-ZM catalyst a promising candidate for the glycerol esterification process and beyond.

Appendix A. Supplementary Material

Supplementary data to this article can be found online at https://doi.org/10.1016/j.cjche.2018.09.013.

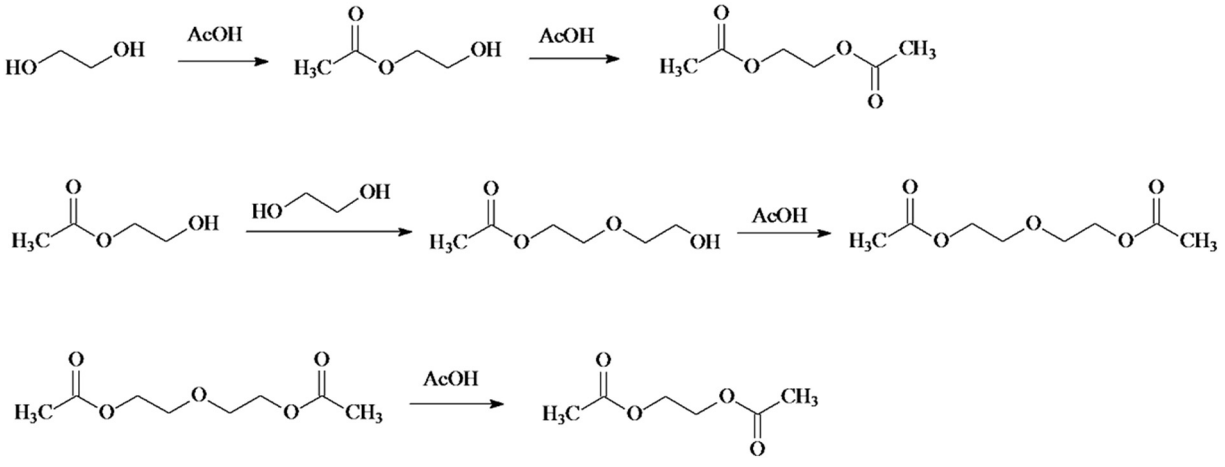

Fig. 6. Reaction scheme for the catalytic esterification of ethylene glycol with acetic acid.

Please cite this article as: J. Liu, *et al.*, Selective synthesis of triacetin from glycerol catalyzed by HZSM-5/MCM-41 micro/mesoporous molecular sieve, *Chin. J. Chem. Eng.* (2018), https://doi.org/10.1016/j.cjche.2018.09.013

References

[1] P.U. Okoye, B.H. Hameed, Review on recent progress in catalytic carboxylation and acetylation of glycerol as a byproduct of biodiesel production, *Renew. Sustain. Energy Rev.* 53 (2016) 558–574.

[2] P.S. Kong, M.K. Aroua, W.M.A.W. Daud, H.V. Lee, P. Cognet, Y. Peres, Catalytic role of solid acid catalysts in glycerol acetylation for the production of bio-additives: A review, *RSC Adv.* 6 (2016) 68885–68905.

[3] X. Wang, P. Zhang, P. Cui, W. Cheng, S. Zhang, Glycerol carbonate synthesis from glycerol and dimethyl carbonate using guanidine ionic liquids, *Chin. J. Chem. Eng.* 25 (2017) 1182–1186.

[4] M. Zhang, Y. Sun, J. Shi, W. Ning, Z. Hou, Selective glycerol oxidation using platinum nanoparticles supported on multi-walled carbon nanotubes and nitrogen-doped graphene hybrid, *Chin. J. Catal.* 38 (2017) 537–544.

[5] D. Wang, Z. Wang, Q. Zhan, Y. Pu, J.-X. Wang, N.R. Foster, L. Dai, Facile and scalable preparation of fluorescent carbon dots for multifunctional applications, *Engineering* 3 (2017) 402–408.

[6] F. Sabri, R. Idem, H. Ibrahim, Metal oxide-based catalysts for the autothermal reforming of glycerol, *Ind. Eng. Chem. Res.* 57 (2018) 2486–2497.

[7] J.F. Chen, Green chemical engineering for a better life, *Engineering* 3 (2017) 279.

[8] Z. Wu, H. Yan, S. Ge, J. Gao, T. Dou, Y. Li, A.C.K. Yip, M. Zhang, MoO_3 modified Ni_2P/Al_2O_3 as an efficient catalyst for crude glycerol to propylene, *Catal. Commun.* 92 (2017) 80–85.

[9] C. Zhang, T. Wang, Y. Ding, One-step synthesis of pyruvic acid from glycerol oxidation over Pb promoted Pt/activated carbon catalysts, *Chin. J. Catal.* 38 (2017) 928–937.

[10] M.T. Liu, L.X. Chen, D.N. Li, A.J. Wang, Q.L. Zhang, J.J. Feng, One-pot controlled synthesis of AuPd@Pd core-shell nanocrystals with enhanced electrocatalytic performances for formic acid oxidation and glycerol oxidation, *J. Colloid Interface Sci.* 508 (2017) 551–558.

[11] P.U. Okoye, A.Z. Abdullah, B.H. Hameed, Synthesis of oxygenated fuel additives via glycerol esterification with acetic acid over bio-derived carbon catalyst, *Fuel* 209 (2017) 538–544.

[12] S.S. Kale, U. Armbruster, R. Eckelt, U. Bentrup, S.B. Umbarkar, M.K. Dongare, A. Martin, Understanding the role of Keggin type heteropolyacid catalysts for glycerol acetylation using toluene as an entrainer, *Appl. Catal. A* 527 (2016) 9–18.

[13] Y. Leng, J. Zhao, P. Jiang, D. Lu, POSS-derived solid acid catalysts with excellent hydrophobicity for highly efficient transformations of glycerol, *Catal. Sci. Technol.* 6 (2016) 875–881.

[14] S. Bagheri, N.M. Julkapli, W.A. Yehye, Catalytic conversion of biodiesel derived raw glycerol to value added products, *Renew. Sustain. Energy Rev.* 41 (2015) 113–127.

[15] L.J. Konwar, P. Mäki-Arvela, P. Begum, N. Kumar, A.J. Thakur, J.-P. Mikkola, R.C. Deka, D. Deka, Shape selectivity and acidity effects in glycerol acetylation with acetic anhydride: selective synthesis of triacetin over Y-zeolite and sulfonated mesoporous carbons, *J. Catal.* 329 (2015) 237–247.

[16] H. Rastegari, H.S. Ghaziaskar, M. Yalpani, Valorization of biodiesel derived glycerol to Acetins by continuous esterification in acetic acid: focusing on high selectivity to Diacetin and Triacetin with no byproducts, *Ind. Eng. Chem. Res.* 54 (2015) 3279–3284.

[17] X. Liao, Y. Zhu, S.-G. Wang, H. Chen, Y. Li, Theoretical elucidation of acetylating glycerol with acetic acid and acetic anhydride, *Appl. Catal. B* 94 (2010) 64–70.

[18] J. Liu, D. Wang, J.-F. Chen, Y. Zhang, Cobalt nanoparticles imbedded into zeolite crystals: a tailor-made catalyst for one-step synthesis of gasoline from syngas, *Int. J. Hydrog. Energy* 41 (2016) 21965–21978.

[19] Y. Wang, Q. Wu, X. Meng, F.-S. Xiao, Insights into the organotemplate-free synthesis of zeolite catalysts, *Engineering* 3 (2017) 567–574.

[20] J. Liu, Z. Wang, P. Jian, R. Jian, Highly selective oxidation of styrene to benzaldehyde over a tailor-made cobalt oxide encapsulated zeolite catalyst, *J. Colloid Interface Sci.* 517 (2018) 144–154.

[21] V.L.C. Gonçalves, B.P. Pinto, J.C. Silva, C.J.A. Mota, Acetylation of glycerol catalyzed by different solid acids, *Catal. Today* 133 (2008) 673–677.

[22] L. Zhou, E. Al-Zaini, A.A. Adesina, Catalytic characteristics and parameters optimization of the glycerol acetylation over solid acid catalysts, *Fuel* 103 (2013) 617–625.

[23] P. Ferreira, I.M. Fonseca, A.M. Ramos, J. Vital, J.E. Castanheiro, Esterification of glycerol with acetic acid over dodecamolybdophosphoric acid encaged in USY zeolite, *Catal. Commun.* 10 (2009) 481–484.

[24] Y. He, Q. Zhang, X. Zhan, D. Cheng, F. Chen, Aluminum impregnated silica catalyst for Friedel–Crafts reaction: Influence of ordering mesostructure, *Chin. J. Chem. Eng.* 25 (2017) 1533–1538.

[25] V. Chaudhary, Sweta, Synthesis and catalytic activity of SBA-15 supported catalysts for styrene oxidation, *Chin. J. Chem. Eng.* 26 (2018) 1300–1306.

[26] J. Liu, S. Fang, R. Jian, F. Wu, P. Jian, Silylated Pd/Ti-MCM-41 catalyst for the selective production of propylene oxide from the oxidation of propylene with cumene hydroperoxide, *Powder Technol.* 329 (2018) 19–24.

[27] A. Patel, S. Singh, A green and sustainable approach for esterification of glycerol using 12-tungstophosphoric acid anchored to different supports: Kinetics and effect of support, *Fuel* 118 (2014) 358–364.

[28] M.S. Khayoon, B.H. Hameed, Synthesis of hybrid SBA-15 functionalized with molybdophosphoric acid as efficient catalyst for glycerol esterification to fuel additives, *Appl. Catal. A* 433 (2012) 152–161.

[29] I. Kim, J. Kim, D. Lee, A comparative study on catalytic properties of solid acid catalysts for glycerol acetylation at low temperatures, *Appl. Catal. B* 148 (2014) 295–303.

[30] J.Y. Liu, J.F. Chen, Y. Zhang, Direct synthesis of Co@Al-MCM-41 catalyst from conventional Co/SiO_2 catalyst, *RSC Adv.* 5 (2015) 62931–62935.

[31] J.Y. Liu, J.F. Chen, Y. Zhang, Cobalt-imbedded zeolite catalyst for direct syntheses of gasoline via Fischer-Tropsch synthesis, *Catal. Sci. Technol.* 3 (2013) 2559–2564.

[32] N. Rahmat, A.Z. Abdullah, A.R. Mohamed, Recent progress on innovative and potential technologies for glycerol transformation into fuel additives: A critical review, *Renew. Sustain. Energy Rev.* 14 (2010) 987–1000.

[33] M.J. Da Silva, N.A. Liberto, L.C. De Andrade Leles, U.A. Pereira, $Fe_4(SiW_{12}O_{40})_3$-catalyzed glycerol acetylation: Synthesis of bioadditives by using highly active Lewis acid catalyst, *J. Mol. Catal. A Chem.* 422 (2016) 69–83.

[34] C. de la Calle, J.M. Fraile, E. Garcia-Bordeje, E. Pires, L. Roldan, Biobased catalyst in biorefinery processes: Sulphonated hydrothermal carbon for glycerol esterification, *Catal. Sci. Technol.* 5 (2015) 2897–2903.

[35] A. P, S.M. Pudi, P. Biswas, Acetylation of glycerol over sulfated alumina: Reaction parameter study and optimization using response surface methodology, *Energy Fuel* 30 (2016) 584–593.

[36] A.B.S. Neto, A.C. Oliveira, E. Rodriguez-Castellón, A.F. Campos, P.T.C. Freire, F.F.F. Sousa, J.M. Filho, J.C.S. Araujo, R. Lang, A comparative study on porous solid acid oxides as catalysts in the esterification of glycerol with acetic acid, *Catal. Today* (2018) https://doi.org/10.1016/j.cattod.2018.05.057.

[37] J. Sun, X. Tong, L. Yu, J. Wan, An efficient and sustainable production of triacetin from the acetylation of glycerol using magnetic solid acid catalysts under mild conditions, *Catal. Today* 264 (2016) 115–122.

[38] M.S. Khayoon, S. Triwahyono, B.H. Hameed, A.A. Jalil, Improved production of fuel oxygenates via glycerol acetylation with acetic acid, *Chem. Eng. J.* 243 (2014) 473–484.

[39] M.S. Khayoon, B.H. Hameed, Acetylation of glycerol to biofuel additives over sulfated activated carbon catalyst, *Bioresour. Technol.* 102 (2011) 9229–9235.

[40] J. Liu, T. Chen, P. Jian, L. Wang, X. Yan, Hollow urchin-like $NiO/NiCo_2O_4$ heterostructures as highly efficient catalysts for selective oxidation of styrene, *J. Colloid Interface Sci.* 526 (2018) 295–301.

Please cite this article as: J. Liu, *et al.*, Selective synthesis of triacetin from glycerol catalyzed by HZSM-5/MCM-41 micro/mesoporous molecular sieve, *Chin. J. Chem. Eng.* (2018), https://doi.org/10.1016/j.cjche.2018.09.013